Short Report

Significant improvement of reprogramming efficiency by transient overexpression of ZGA inducer Dux but not Dppa2/4

Lei Yang[1], Xuefei Liu[1], Lishuang Song[1, 2], Anqi Di[1, 2], Guanghua Su[1, 2], Chunling Bai[1, 2], Zhuying Wei[1, 2], and Guangpeng Li[1, 2, *]

1 State Key Laboratory of Reproductive Regulation and Breeding of Grassland Livestock (R^2BGL), Inner Mongolia University, Hohhot 010070, China.

2 College of Life Sciences, Inner Mongolia University, Hohhot 010070, China.

* Correspondence: Guangpeng Li (gpengli@imu.edu.cn)

Abstract

Cloned animal have been reported by somatic cell nuclear transfer (SCNT) for many years. However, the SCNT is extremely inefficient, and zygotic genome activation (ZGA) is required for SCNT and chemical mediated reprogramming. To identify candidate factors that facilitate ZGA in reprogramming, we performed siRNA-repressor and mRNA-inducer screening, which revealed Dux, Dppa2, and Dppa4 as key factors enhancing the ZGA in SCNT. Direct injection of ZGA-inducers had no significant effect on the SCNT blastocyst formation, and even destroyed the ZGA. Through a inducible Dux transgenic mouse model, we demonstrate that transient overexpression of Dux not only improved SCNT efficiency, but also increased the efficiency of chemical reprogramming. Transcriptome profiling revealed that Dux treated SCNT embryos were similar to fertilized embryos. Furthermore, transient overexpression of Dux combined with inactivation of DNA methyltransferases (Dnmts) further promote the overall development of SCNT-derived animals. These findings enhance our understanding of ZGA-regulators in somatic reprogramming.

Introduction

The scientists at the Institute of Neuroscience (Chinese Academy of Sciences), recently cloned the world's first monkeys Zhong Zhong and Hua Hua (the Zhong Hua is a mandarin term for china) (Z. Liu et al., 2018). After the first mammal Dolly sheep to be cloned (Wilmut, Schnieke, McWhir, Kind, & Campbell, 1997), the created non-human primate has once again attracted worldwide attention. Indeed, successful cloning of the sheep and monkey not only made reproductive cloning possible, but also raised the possibility of therapeutic cloning. Somatic cell nuclear transfer (SCNT) is the technical term for cloning in which terminal differentiated somatic cell is transferred into enucleated oocyte, in which the cytoplasmic factors reprogram the nucleus to become a zygote-like state (Matoba & Zhang, 2018). Both SCNT derived and Yamanaka factors induced pluripotent stem (iPS) cells have the potential to generate patient-specific pluripotent stem cells for replacement therapy. Compared with iPS, the SCNT reprogramming is oncogene-free methodologies. Thus, SCNT derived pluripotent stem cells would be more suitable for human therapeutic applications.

Following fertilization, the newly formed zygotic genome is activated through a process known as the zygotic genome activation (ZGA), which enables zygote can subsequently development to the adult animal (Lu & Zhang, 2015). A similar mechanism is likely used in ZGA of SCNT embryos (T. Gao et al., 2007; Matoba & Zhang, 2018). Indeed, our and others recent results have revealed that incomplete ZGA is a major reprogramming barrier (W. Liu et al., 2016; Matoba et al., 2014; Wang et al., 2018; Yang, Song, Liu, Bai, & Li, 2018). Although many advances have been made in SCNT technology via different epigenetic regulators, the SCNT for producing cloned animals still inefficient.

The transcription factor of double homeobox (Dux) was identified as a key inducer of ZGA in normal fertilized embryos (De Iaco et al., 2017; Hendrickson et al., 2017; Whiddon, Langford, Wong, Zhong, & Tapscott, 2017). Very recently, two independent studies found that transcription factors developmental pluripotency associated 2 (Dppa2) and Dppa4 are both

necessary and sufficient for the activation of ZGA (De Iaco, Coudray, Duc, & Trono, 2019; Eckersley-Maslin et al., 2019). Therefore, as far as we know, at least three factors can be called master ZGA-inducer in fertilized embryos. Furthermore, overexpression of Dux is sufficient to drive pluripotent stem cells into a totipotent state by expressing 2-cell embryo specific transcripts (2-cell-like stem cells) (Macfarlan et al., 2012). In addition, several studies show totipotent state that the be achieved by depleting ZGA-repressor, such as tripartite motif-containing 28 (Trim28) (Rodriguez-Terrones et al., 2018), microRNA 34a (miR-34a) (Choi et al., 2017), chromatin assembly factor (CAF-1) (Ishiuchi et al., 2015), lysine (K)-specific demethylase 1A (Lsd1/Kdm1a) (Ancelin et al., 2016; Macfarlan et al., 2012; Wasson et al., 2016), and long interspersed nuclear element (LINE1) (Percharde et al., 2018).

The effect of ZGA-regulators in somatic cell reprograming remains unknown. Thus, the aims of this study were to explore the relationship between ZGA-regulator and SCNT efficiency, and to identify a smart factor that could promotes the efficiency of somatic reprogramming.

Results and Discussion

We have recently established a MERVL::tdTomato based ZGA real-time monitor system (Yang et al., 2018). To identify candidate factors that facilitate ZGA in SCNT reprogramming, we carried out a siRNA-repressor and mRNA-inducer screening in SCNT (Figure 1A). From the screen, we identified a number of factors that when over-expression or knock-down resulted in reporter activation (supplement Figure S1A). Among the identified factors, Dux, Dppa2, and Dppa4 showed the strongest phenotype (Figure 1B and C). Intriguingly, we found that most SCNT embryos injected with Dppa2 or Dppa4 mRNA arrested at the 1-cell stage (called '1-cell block' for simplicity; Figure 1D and E; supplement Figure S1B, Movie S1, S2). Direct injection of Dux mRNAs had no significant impact on the blastocyst formation rate (*vs.* canonical SCNT; 21.2% *vs.* 23.6%; Figure 1D; supplement Table S1). Indeed, direct injection of Dux will increase the rate of SCNT embryo fragmentation (Figure 1D and E; supplement Movie S2). Nevertheless, when Dux was over-expressed in SCNT embryos, the rate of 2-cell

82 block was significantly reduced (Figure 1D). These results suggest that Dux (but not Dppa2/4)
83 is a key factor whose overexpression can rescue 2-cell arrest in SCNT embryos.
84
85 It is known that ZGA is governed by a time-dependent 'zygotic clock' (i.e. 24h post-fertilization),
86 and Dux is expressed as a brief pulse in early 2-cell stage (De Iaco et al., 2019; Eckersley-
87 Maslin et al., 2019; Rodriguez-Terrones et al., 2018). Therefore, we wonder whether Dux is
88 time-depend on improving the efficiency of SCNT embryo development. To answer this
89 question, we generated transgenic mouse lines containing doxycycline (dox) inducible Dux
90 gene (supplement Figure S2A-B). By switching the culture medium between dox-containing
91 and -lacking at various time points, the critical period for the dox-Dux requirement was mapped
92 to a 24-h window (Figure 1F). When the dox was supplied in this window, the SCNT blastocyst
93 formation rate was significantly increased (Figure 1G; supplement Table S2). Subsequently,
94 we performed single-cell RNA sequencing (scRNA-seq) to examine the possible changes of
95 the ZGA related gene expressions in Dux-overexpressed 2-cell SCNT embryos (D-SCNT).
96 Unsupervised hierarchal clustering revealed that the ICSI and D-SCNT generated embryos in
97 the same cluster, and ZGA-genes were upregulated in D-SCNT embryos (Figure 1H and I;
98 supplement Figure S3A-D; Dataset S1, S2). These results indicating the improvement of Dux
99 on SCNT embryonic development depends on its treatment time.
100
101 The SCNT blastocyst rate was improved by injecting Kdm4d mRNA (K-SCNT) (Matoba et al.,
102 2014). We next compared the developmental potential of SCNT embryos derived by K-SCNT
103 and D-SCNT. We found that the blastocyst formation rate of D-SCNT was similar to K-SCNT
104 (84.72% *vs.* 86.79%; supplement Figure S4A, Table S2). Nonetheless, the cloned pup birth
105 rate of D-SCNT was higher than K-SCNT (10.71% *vs.* 7.81%; Figure 1J; supplement Table
106 S3). Despite D-SCNT or K-SCNT, the abnormally large placentas are still observed in those
107 cloned pups (supplement Figure S4B, Table S3). Previous studies have indicated that knock-
108 down DNA-methyltransferases Dnmt3a/b led to less placental abnormalities (Si-SCNT) (R.
109 Gao et al., 2018). We next investigated whether combined D-SCNT and Si-SCNT could further

110 improve SCNT embryonic development. Compared with canonical SCNT, combined K-SCNT
111 and Si-SCNT improved the pup birth-rate from 1.01% to 12.24%, but less than D-SCNT
112 combined with Si-SCNT (18.60%; Figure 1J). Genotyping analysis confirmed that all the
113 cloned pups were generated from donor cells (supplement Figure S4C). The large placental
114 phenotype was rescued by the D-Si-SCNT combined approach (supplement Figure S4B).
115
116 Deng et al. identified a unique embryonic 2-cell like status as the key molecular event that led
117 to successful chemical reprogramming (CiPS) (Zhao et al., 2018). Thus, we tried to improve
118 the CiPS by overexpression of ZGA inducer Dux (D-CiPS). The dox-inducible mouse
119 embryonic fibroblasts (dDux-MEFs) cells were isolated from the transgenic mice. As shown in
120 Figure 2A, we treated the dDux-MEFs with dox for various durations, and observed that Dux
121 displayed remarkable effect at the stage-2 of CiPS. About 36 alkaline phosphatase-positive
122 (AP_+) colonies could be observed in D-CiPS wells (starting from 50,000 MEFs per well of 6-
123 well plate), while only 26 AP_+ colonies could be observed in the canonical CiPS well (Figure
124 2B and C). Consistently, the ZGA related genes were significantly upregulated after transient
125 expression of Dux (Figure 2D). These D-CiPS induced cells were pluripotent as demonstrated
126 by standard characterization procedures (Figure 2E-G). We found, based on bisulfite
127 sequencing, that successful demethylation occurred in the promoters of Oct4 and Nanog in
128 the D-CiPS induced cell lines (Figure 2H).
129
130 When we prepare this manuscript, two recent studies suggested that Dux is important but not
131 essential for fertilized embryo development by enhancing rather than ZGA inducer (Chen &
132 Zhang, 2019; Guo et al., 2019). However, we demonstrate here that transient overexpression
133 of ZGA-inducer Dux not only improved SCNT efficiency, but also increased the efficiency of
134 chemical reprogramming. Ectopic expression of Dppa2/4 in SCNT embryos resulted in 1-cell
135 block, which implied that successful timely ZGA is essential for the development of SCNT-
136 derived embryos. A recent study found that Dppa2/4 interacted with small ubiquitin-like
137 modifier (SUMO) related proteins (Yan et al., 2019). Therefore, we speculated that

138 overexpression of Dppa2/4 would accelerate the degradation of reprogramming factors in the
139 oocyte-cytoplasm, which leads to reprogramming failure. Nonetheless, fertilized embryos
140 completely differ from SCNT-derived embryos. SCNT embryos are generated by directly
141 injecting somatic nuclei into enucleated oocytes, whereas the oocyte cytoplasm is
142 evolutionally designed to reprogram the spermatozoa. Therefore, although Dux and Dppa2/4
143 as ZGA-inducers, its effects on the reprogramming process likely differ between sperm and
144 somatic cells. Thus, the relationship among Dux, Dppa2/4, and ZGA in SCNT warrants further
145 investigation.
146
147 Overall, our study revealed that transient overexpression of Dux not only improved SCNT
148 efficiency, but also increased the efficiency of chemical reprogramming. The Dux was
149 identified as a ZGA-inducer in mouse, human, and likely all mammalian animals (Iturbide &
150 Torres-Padilla, 2017; Whiddon et al., 2017). Thus, we reasoned that transient overexpression
151 of Dux could also improves reprogramming efficiency of all mammals.
152

153 **Materials and methods**

154 **Animals and Chemicals**

155 Specific pathogen-free (SPF)-grade BDF1 (C57BL/6N × DBA/2), CD1, and Kun-Ming (KM)
156 mice mice were purchased from Laboratory Animal Research Center (Inner Mongolia
157 University) or Vital River Laboratories (Beijing, China). All animal experiments were approved
158 by the Animal Care and Use Committee of Inner Mongolia University. All procedures were
159 carried out in strict accordance with the recommendations made in the Guide for the Care and
160 Use of Laboratory Animals of the National Veterinary and Quarantine Service. MERLV::
161 tdTomato transgenic mice, which carry a transgenic MERLV promoter LTR driven tdTomato
162 reporter (Yang et al., 2018), were mated with the same positive mice. dDux-MEFs cells were
163 isolated from E12.5 fetus. The MERLV:: tdTomato embryos used in the experiment were
164 produced by MERVL::tdTomato sperm and MII oocytes from the littermates of transgenic mice.
165 All chemicals used in this study were purchased from Sigma (USA), unless otherwise
166 indicated.

167

168 **SCNT and embryo culture**

169 The SCNT processes followed previously published studies (Kishigami et al., 2006; Yang et
170 al., 2018). Briefly, groups of ~50 MII oocytes were transferred to a chamber containing oil-
171 covered M2 supplemented with 5 μg/ml cytochalasin B (CB). The spindle-chromosome
172 complex (SCC) was removed by a blunt Piezo-driven pipette (~10 μm internal diameter) on a
173 37°C heating stage of an inverted microscope (Nikon, Japan). The nuclei of donor cells were
174 drawn in and out of the injection pipette until its plasma membrane was broken and was then
175 injected into enucleated oocytes. The reconstructed embryos were cultured in aMEM medium
176 (Thermo, USA) containing 10% fetal calf serum (FCS; Hyclone, USA) for 1 h before activation
177 treatment. The reconstructed embryos were activated in Ca^{2+} free KSOM medium containing
178 10 mM strontium and 5 μg/ml CB for 6 h. Activated embryos were thoroughly washed and
179 cultured in G1/G2 medium (1:1, vol / vol; Vitrolife, Sweden). Induction of Dux was performed
180 by administration of doxycycline (2 μg/ml) in the G1/G2 medium.

181

182 **Immunofluorescence staining**

183 Embryos and CiPS cells were rinsed three times in phosphate-buffered saline (PBS) with 0.3%
184 BSA, fixed with 4% paraformaldehyde (PFA) overnight at 4°C, and then permeabilized with
185 0.2% (vol / vol) Triton X-100 for 15 min at room temperature, followed by washing thoroughly
186 in PBS containing 0.3% BSA. Fixed samples were blocked in 0.05% Tween 20 in PBS
187 containing 3% BSA (PBST) at 37°C for 1 h and then incubated with the primary antibodies
188 overnight at 4°C. Samples were incubated with primary antibodies against HA (Santa Cruz,
189 sc-7392, USA), Oct4 (Santa Cruz, sc-8629, USA), and Ssea1 (Santa Cruz, sc-21702, USA).
190 After incubating, the samples were needed to wash several times in PBST and then incubated
191 with appropriate secondary antibodies conjugated with Alexa Fluor 594 and Alexa Fluor 488
192 (Thermo, USA) for 1 h at 37°C. For imaging, the embryos were mounted in 10 μl anti-fade
193 solution with DAPI (Thermo, USA) and compressed with a cover-slip. All samples were
194 observed by laser scanning microscope (Nikon, Japan).

195

196 ***In vitro* mRNA synthesis and microinjection in oocytes**

197 The *Dux*, *Dppa2*, and *Dppa4* mRNA were cloned into T7-driven vectors, and mRNAs were
198 synthetized *in vitro* using mMESSAGE mMACHINE T7 Ultra Kit (Thermo, USA) following the
199 manufacturer's instructions. The integrity of manufactured mRNA was confirmed by
200 electrophoresis with formaldehyde gels. The final concentration of mRNA was diluted to 900
201 ng/ml before injection. As previously described (Yang et al., 2018), 8 pl of mRNA was
202 microinjected into the cytoplasm of denuded oocytes. These oocytes were obtained by
203 superovulating BDF1 female mice by intraperitoneal injection of 10 IU pregnant mare serum
204 gonadotropin (PMSG; Sansheng, China) and 10 IU human chorionic gonadotropin (hCG;
205 Sansheng, China) 48 h apart. The cumulus-oocyte complexes (COCs) were collected from
206 oviducts 14 h post-hCG, and the cumulus cells were dispersed by EmbryoMax FHM Mouse
207 Embryo Media (Millipore, USA). Oocytes were injected using Piezo-operated blunt-end
208 micropipette (3~5 μm internal diameter). After injection, oocytes were kept at room-

209 temperature for 30 min and then moved into the incubator. The siRNA information was
210 presented in Table S4.
211
212 **Generation of CiPS cells**
213 This section was adapted from Deng's lab (Zhao et al., 2018). Reagents setup: Small
214 molecules: VPA, CHIR99021, 616452, Tranylcypromine, Forskolin, Ch55, EPZ004777,
215 DZNep, Decitabine, SGC0946, and PD0325901. Stage I medium: FBS/KSR-based medium
216 supplemented with the small-molecule cocktail VC6TF5E (100 μM VPA, 40 μM CHIR99021,
217 10 μM 616452, 5 μM Tranylcypromine, 10 μM Forskolin, 1 μM Ch55, and 5 μM EPZ004777).
218 N2B27-SII medium: N2B27-based medium supplemented with 10 ng/ml LIF, 50 μg/ml vitamin
219 C, 25 ng/ml bFGF, 2 mg/ml Albumax-II, and the small-molecule cocktail VC6TF5ZDS (VPA at
220 1 mM). Stage III medium: N2B27-based medium with 3 μM CHIR99021, 1 μM PD0325901,
221 10 ng/ml LIF, and 50 μg/ml vitamin C. On day –1, MEFs were seeded at 50,000 cells per well
222 of 6-well plate with MEF culture medium. The next day (day 0), change the medium into
223 optimized stage I medium. From day 6~12, cells were cultured in optimized N2B27-SII medium.
224 During day 12~16, cells were cultured in stage III medium with 500 μM VPA. On day 16, VPA
225 was removed and cells were cultured in stage III medium. After another 4~10 days, CiPS
226 colonies emerged. Induction of Dux was performed by administration of doxycycline (2 μg/ml)
227 in the culture medium.
228
229 **Transgenic mice generation**
230 The pCW57.1-mDux-CA vector was a gift from Stephen Tapscott (Addgene 99284). The
231 pronuclear microinjection for the production of transgenic mice followed previously published
232 studies (Ittner & Gotz, 2007). Briefly, the vector was injected into the well-recognized pronuclei.
233 Injected zygotes were transferred into pseudopregnant female mice (~ 30 zygotes per mouse)
234 after 4 h recovery culture in KSOM-AA medium (Millipore, USA). For founder identification, tail
235 tips were subjected to standard DNA extraction procedures. The amplified DNA fragments
236 were subjected to TA cloning and sequencing. The founder mice were crossed to the

237 littermates of founder mice for four generations to produce homozygous Dux mice.

238

239 **Alkaline phosphatase staining**

240 For alkaline phosphatase staining, CiPS cells were fixed with 4% PFA in PBS for 2 min, rinsed
241 once with PBS and detection was performed using a Alkaline Phosphatase Assay Kit
242 (VECTOR, USA) according to the manufacturer's protocol.

243

244 **Real-time qPCR analysis**

245 Total RNA was isolated using TRIzol reagent (Thermo, USA) and was immediately reverse-
246 transcribed using a Prime Script RT reagent kit (Takara, Japan). The reverse transcription
247 PCR was were amplified using Ex Taq (Takara, Japan). The qPCR was performed using a
248 SYBR Premix Ex Taq (Takara, Japan) and signals were detected with Applied Biosystems
249 7500 real-time PCR System (Thermo, USA). Relative mRNA expression was calculated use
250 the $2^{(-\Delta\Delta Ct)}$ method. The primer information was presented in Table S5.

251

252 **Chimeric mice and embryo transfer**

253 For chimeric experiments, CiPS cells were used one day before passaging, which showed an
254 optimal undifferentiated morphology. The CiPS cells were microinjected into CD1/KM
255 blastocysts using a Piezo (Primetech, Japan) microinjection pipette. After culturing for 3 h, the
256 embryos were transplanted into the uterus of pseudopregnant mice (~15 embryos per mouse).
257 The 2-cell stage SCNT embryos were transferred to the oviducts of E0.5 pseudopregnant (~20
258 embryos per mouse). The cloned pups nursed by lactating CD1/KM females. SSLP analysis
259 was performed for D6Mit15 and D2Mit102. The primer information is presented in Table S5.

260

261 **Teratoma formation**

262 Teratoma formation analysis was carried out to evaluate the pluripotency of CiPS cells.
263 Approximately 10^6 CiPS cells were injected subcutaneously into the hind limbs of a 8-week-
264 old nude mice. After 6 weeks, fully formed teratomas were dissected and fixed with PBS

265 containing 4% PFA, then embedded in paraffin, sectioned and stained with haematoxylin and
266 eosin for histological analysis.
267
268 **Bisulfite genomic sequencing**
269 Genomic DNA was extracted by the tissue & blood DNA extraction kit (Qiagen, Germany) and
270 treated with the Methylamp DNA modification kit (Epigentek, USA). The bisulphite conversion
271 was performed as previously published studies (Cao et al., 2018).
272
273 **RNA-sequencing**
274 The single-cell RNA-seq method followed previously published studies (W. Liu et al., 2016;
275 Tang et al., 2010). The reverse transcription was performed directly on the cytoplasmic lysate
276 of individual embryos. The total cDNA library was then amplified by 18~20 cycles for library
277 construction, which was performed following manufacturer's instructions (Illumina, USA).
278 Paired-end sequencing was further performed at Annoroad (Beijing, China). Three biological
279 replicates were analyzed for each treatment condition. After removing low-quality reads and
280 adapters, the raw reads were mapped to the mm9 genome using Tophat (v1.3.3) with default
281 parameters (Trapnell, Pachter, & Salzberg, 2009). Expression levels for all RefSeq transcripts
282 were quantified to fragments per kilobase of exon model per million mapped reads (FPKM)
283 using Cufflinks (v1.2.0) (Trapnell et al., 2010). Gene Ontology (GO) analyses for differentially
284 expressed genes were performed by using the R package GO.db and Database for Annotation,
285 Visualization and Integrated Discovery (DAVID) (Huang da, Sherman, & Lempicki, 2009).
286
287 **Statistics analysis and data availability**
288 Statistical analyses were done using the univariate analysis of variance (ANOVA) followed by
289 the Student t-test with SPSS 21.0 statistical software (Armonk, USA). $P < 0.05$ was considered
290 significant. Sequencing data have been deposited in the NCBI sequence read archive (SRA)
291 under accession codes: SCNT-1 (SAMN12871322), SCNT-2 (SAMN12871323), SCNT-3
292 (SAMN12871324); D-SCNT-1 (SAMN12871325), D-SCNT-2 (SAMN12871326), D-SCNT-3

(SAMN12871327); ICSI-1 (SAMN12871328), ICSI-2 (SAMN12871329), ICSI-3 (SAMN12871330).

Acknowledgements

We thank Prof. Shaorong Gao (Tongji University), Prof. Zhiming Han (Chinese Academy of Sciences), and Prof. Qing Xia (Peking University) for their technical assistance. We also thank Prof. Yi Zhang (Harvard Medical School) for sharing the list of RRRs. This study was supported by the Genetically Modified Organisms Breeding Major Projects (2016ZX08007-002), the opening project of State Key Laboratory of R2BGL (to L.Y.), the Inner Mongolia University Chief Scientist Program (to G.L.), the Inner Mongolia Autonomous Region Basic Research Project (to G.L.).

Author contributions

L.Y. and G.L. conceived and designed the study. L.Y., X.L., L.S., A.D., G.S., C.B., and Z.W. performed the experiments. L.Y., X.L., L.S., A.D., and G.S. analyzed the data. G.L. supervised the project. L.Y. and G.L. wrote the paper.

Competing interests

The authors declare no competing interests.

References

Ancelin, K., Syx, L., Borensztein, M., Ranisavljevic, N., Vassilev, I., Briseno-Roa, L., . . . Heard, E. (2016). Maternal LSD1/KDM1A is an essential regulator of chromatin and transcription landscapes during zygotic genome activation. *Elife, 5*, e08851. doi:10.7554/eLife.08851

Cao, S., Yu, S., Li, D., Ye, J., Yang, X., Li, C., . . . Pei, D. (2018). Chromatin accessibility dynamics during chemical induction of pluripotency. *Cell Stem Cell, 22*(4), 529-542. doi:10.1016/j.stem.2018.03.005

Chen, Z., & Zhang, Y. (2019). Loss of DUX causes minor defects in zygotic genome activation and is compatible with mouse development. *Nat Genet, 51*(6), 947-951. doi:10.1038/s41588-019-0418-7

Choi, Y. J., Lin, C. P., Risso, D., Chen, S., Kim, T. A., Tan, M. H., . . . He, L. (2017). Deficiency of microRNA miR-34a expands cell fate potential in pluripotent stem cells. *Science, 355*(6325), eaag1927. doi:10.1126/science.aag1927

De Iaco, A., Coudray, A., Duc, J., & Trono, D. (2019). DPPA2 and DPPA4 are necessary to establish a 2C-like state in mouse embryonic stem cells. *EMBO Rep, 20*(5), e47382. doi:10.15252/embr.201847382

De Iaco, A., Planet, E., Coluccio, A., Verp, S., Duc, J., & Trono, D. (2017). DUX-family transcription factors regulate zygotic genome activation in placental mammals. *Nat Genet, 49*(6), 941-945. doi:10.1038/ng.3858

Eckersley-Maslin, M., Alda-Catalinas, C., Blotenburg, M., Kreibich, E., Krueger, C., & Reik, W. (2019). Dppa2 and Dppa4 directly regulate the Dux-driven zygotic transcriptional program. *Genes Dev, 33*(3-4), 194-208. doi:10.1101/gad.321174.118

Gao, R., Wang, C., Gao, Y., Xiu, W., Chen, J., Kou, X., . . . Gao, S. (2018). Inhibition of aberrant DNA re-methylation improves post-implantation development of somatic cell nuclear transfer embryos. *Cell Stem Cell, 23*(3), 426-435. doi:10.1016/j.stem.2018.07.017

Gao, T., Zheng, J., Xing, F., Fang, H., Sun, F., Yan, A., . . . Sheng, H. Z. (2007). Nuclear reprogramming: the strategy used in normal development is also used in somatic cell nuclear transfer and parthenogenesis. *Cell Res, 17*(2), 135-150. doi:10.1038/cr.2007.2

Guo, M., Zhang, Y., Zhou, J., Bi, Y., Xu, J., Xu, C., . . . Wang, Y. (2019). Precise temporal regulation of Dux is important for embryo development. *Cell Res*, Published online 2019-Oct-7. doi:10.1038/s41422-019-0238-4

Hendrickson, P. G., Dorais, J. A., Grow, E. J., Whiddon, J. L., Lim, J. W., Wike, C. L., . . .

Cairns, B. R. (2017). Conserved roles of mouse DUX and human DUX4 in activating cleavage-stage genes and MERVL/HERVL retrotransposons. *Nat Genet, 49*(6), 925-934. doi:10.1038/ng.3844

Huang da, W., Sherman, B. T., & Lempicki, R. A. (2009). Systematic and integrative analysis of large gene lists using DAVID bioinformatics resources. *Nat Protoc, 4*(1), 44-57. doi:10.1038/nprot.2008.211

Ishiuchi, T., Enriquez-Gasca, R., Mizutani, E., Boskovic, A., Ziegler-Birling, C., Rodriguez-Terrones, D., . . . Torres-Padilla, M. E. (2015). Early embryonic-like cells are induced by downregulating replication-dependent chromatin assembly. *Nat Struct Mol Biol, 22*(9), 662-671. doi:10.1038/nsmb.3066

Ittner, L. M., & Gotz, J. (2007). Pronuclear injection for the production of transgenic mice. *Nat Protoc, 2*(5), 1206-1215. doi:10.1038/nprot.2007.145

Iturbide, A., & Torres-Padilla, M. E. (2017). Starting embryonic transcription for the first time. *Nat Genet, 49*(6), 820-821. doi:10.1038/ng.3880

Kishigami, S., Wakayama, S., Thuan, N. V., Ohta, H., Mizutani, E., Hikichi, T., . . . Wakayama, T. (2006). Production of cloned mice by somatic cell nuclear transfer. *Nat Protoc, 1*(1), 125-138. doi:10.1038/nprot.2006.21

Liu, W., Liu, X., Wang, C., Gao, Y., Gao, R., Kou, X., . . . Gao, S. (2016). Identification of key factors conquering developmental arrest of somatic cell cloned embryos by combining embryo biopsy and single-cell sequencing. *Cell Discov, 2*, 16010. doi:10.1038/celldisc.2016.10

Liu, Z., Cai, Y., Wang, Y., Nie, Y., Zhang, C., Xu, Y., . . . Sun, Q. (2018). Cloning of macaque monkeys by somatic cell nuclear transfer. *Cell, 172*(4), 881-887. doi:10.1016/j.cell.2018.01.020

Lu, F., & Zhang, Y. (2015). Cell totipotency: molecular features, induction, and maintenance. *Natl Sci Rev, 2*(2), 217-225. doi:10.1093/nsr/nwv009

Macfarlan, T. S., Gifford, W. D., Driscoll, S., Lettieri, K., Rowe, H. M., Bonanomi, D., . . . Pfaff, S. L. (2012). Embryonic stem cell potency fluctuates with endogenous retrovirus activity. *Nature, 487*(7405), 57-63. doi:10.1038/nature11244

Matoba, S., Liu, Y., Lu, F., Iwabuchi, K. A., Shen, L., Inoue, A., & Zhang, Y. (2014). Embryonic development following somatic cell nuclear transfer impeded by persisting histone methylation. *Cell, 159*(4), 884-895. doi:10.1016/j.cell.2014.09.055

Matoba, S., & Zhang, Y. (2018). Somatic cell nuclear transfer reprogramming: mechanisms

379 and applications. *Cell Stem Cell, 23*(4), 471-485. doi:10.1016/j.stem.2018.06.018
380 Percharde, M., Lin, C. J., Yin, Y., Guan, J., Peixoto, G. A., Bulut-Karslioglu, A., . . . Ramalho-
381 Santos, M. (2018). A LINE1-nucleolin partnership regulates early development and
382 ESC identity. *Cell, 174*(2), 391-405. doi:10.1016/j.cell.2018.05.043
383 Rodriguez-Terrones, D., Gaume, X., Ishiuchi, T., Weiss, A., Kopp, A., Kruse, K., . . . Torres-
384 Padilla, M. E. (2018). A molecular roadmap for the emergence of early-embryonic-like
385 cells in culture. *Nat Genet, 50*(1), 106-119. doi:10.1038/s41588-017-0016-5
386 Tang, F., Barbacioru, C., Nordman, E., Li, B., Xu, N., Bashkirov, V. I., . . . Surani, M. A. (2010).
387 RNA-Seq analysis to capture the transcriptome landscape of a single cell. *Nat Protoc,*
388 *5*(3), 516-535. doi:10.1038/nprot.2009.236
389 Trapnell, C., Pachter, L., & Salzberg, S. L. (2009). TopHat: discovering splice junctions with
390 RNA-seq. *Bioinformatics, 25*(9), 1105-1111. doi:10.1093/bioinformatics/btp120
391 Trapnell, C., Williams, B. A., Pertea, G., Mortazavi, A., Kwan, G., van Baren, M. J., . . . Pachter,
392 L. (2010). Transcript assembly and quantification by RNA-seq reveals unannotated
393 transcripts and isoform switching during cell differentiation. *Nat Biotechnol, 28*(5), 511-
394 515. doi:10.1038/nbt.1621
395 Wang, Y., Zhao, C., Hou, Z., Yang, Y., Bi, Y., Wang, H., . . . Gao, S. (2018). Unique molecular
396 events during reprogramming of human somatic cells to induced pluripotent stem cells
397 (iPSCs) at naive state. *Elife, 7*, e29518. doi:10.7554/eLife.29518
398 Wasson, J. A., Simon, A. K., Myrick, D. A., Wolf, G., Driscoll, S., Pfaff, S. L., . . . Katz, D. J.
399 (2016). Maternally provided LSD1/KDM1A enables the maternal-to-zygotic transition
400 and prevents defects that manifest postnatally. *Elife, 5*, e08848.
401 doi:10.7554/eLife.08848
402 Whiddon, J. L., Langford, A. T., Wong, C. J., Zhong, J. W., & Tapscott, S. J. (2017).
403 Conservation and innovation in the DUX4-family gene network. *Nat Genet, 49*(6), 935-
404 940. doi:10.1038/ng.3846
405 Wilmut, I., Schnieke, A. E., McWhir, J., Kind, A. J., & Campbell, K. H. (1997). Viable offspring
406 derived from fetal and adult mammalian cells. *Nature, 385*(6619), 810-813.
407 doi:10.1038/385810a0
408 Yan, Y. L., Zhang, C., Hao, J., Wang, X. L., Ming, J., Mi, L., . . . Wang, Y. (2019). DPPA2/4 and
409 SUMO E3 ligase PIAS4 opposingly regulate zygotic transcriptional program. *PLoS Biol,*
410 *17*(6), e3000324. doi:10.1371/journal.pbio.3000324
411 Yang, L., Song, L., Liu, X., Bai, L., & Li, G. (2018). KDM6A and KDM6B play contrasting roles

412 in nuclear transfer embryos revealed by MERVL reporter system. *EMBO Rep, 19*(12),
413 e46240. doi:10.15252/embr.201846240
414 Zhao, T., Fu, Y., Zhu, J., Liu, Y., Zhang, Q., Yi, Z., . . . Deng, H. (2018). Single-cell RNA-seq
415 reveals dynamic early embryonic-like programs during chemical reprogramming. *Cell*
416 *Stem Cell, 23*(1), 31-45. doi:10.1016/j.stem.2018.05.025
417

418 **Figure legends**

419 **Figure 1. Dux act as promote factors for SCNT-mediated somatic cell reprogramming.**

420 (A) Schematic illustration of the screen strategy.

421 (B) Quantification of embryos that expression ZGA reporter (MERVL::tdTomato) after injection
422 with siRNA-repressor or mRNA- inducer. N, total number of embryos analyzed for each
423 condition. Error bars, mean ± S.D.; three independent experiment replicates were
424 performed.

425 (C) Representative fluorescence image of SCNT embryos derived by different methods. The
426 SCNT embryos produced by transfer of MERVL::tdTomato cumulus cell into WT
427 enucleated oocytes. Scale bar, 100 μm.

428 (D) Stacked bar plots show fraction of embryos at blastocyst stages after injection with
429 different mRNA as indicated. N, total number of embryos analyzed for each condition.

430 (E) Representative live-cell images of dynamics ZGA reporter expression during SCNT
431 embryos development. The time after starting observation is shown on the bottom of
432 image. Scale bar, 50 μm.

433 (F) Schematic transient induction of Dux. All timings reported in this paper is hour post-
434 activation.

435 (G) The preimplantation development of SCNT embryos. Shown is the percentage of embryos
436 that reaches each indicated stage. Scale bar, 100 μm.

437 (H) Unsupervised hierarchical clustering.

438 (I) Venn diagram showing the overlap between the genes that failed to be activated in SCNT
439 2-cell embryos and derepressed in D-SCNT. Heatmap, GO terms showing the expression
440 pattern of 257 overlap genes.

441 (J) The birth rate of SCNT embryos derived by different methods.

442

443 **Figure 2. Dux facilitates chemical-mediated somatic cell reprogramming.**

444 (A) Durations of dox addition at different time points during chemical induction (left) and
445 assessment of AP_+ colonies (right). Error bars, mean ± S.D.

446 (B) Morphological changes at distinct time points during D-CiPS. Scale bar, 100 μm.

447 (C) Representative images of the number of AP_+ positive colonies.

448 (D) Relative expression levels by qPCR of select ZGA genes in D-CiPS, compared with

449 canonical CiPS. Error bars, S.E.M.; n = 3; ***P < 0.001 by Student's t-test.

450 (E) Immunostaining images of D-CiPS expressed pluripotency markers. Scale bar, 50 μm.

451 (F) Histology by H&E staining of teratoma tissues derived by D-CiPS cells. Scale bar, 200 μm.

452 (G) Chimeric mouse generated from D-CiPS cells.

453 (H) Bisulfite sequencing analysis of Oct4 and Nanog demethylation in D-CiPS or canonical

454 CiPS cells (filled squares are methylated CpGs and empty ones indicate unmethylated).

455

Fig.1

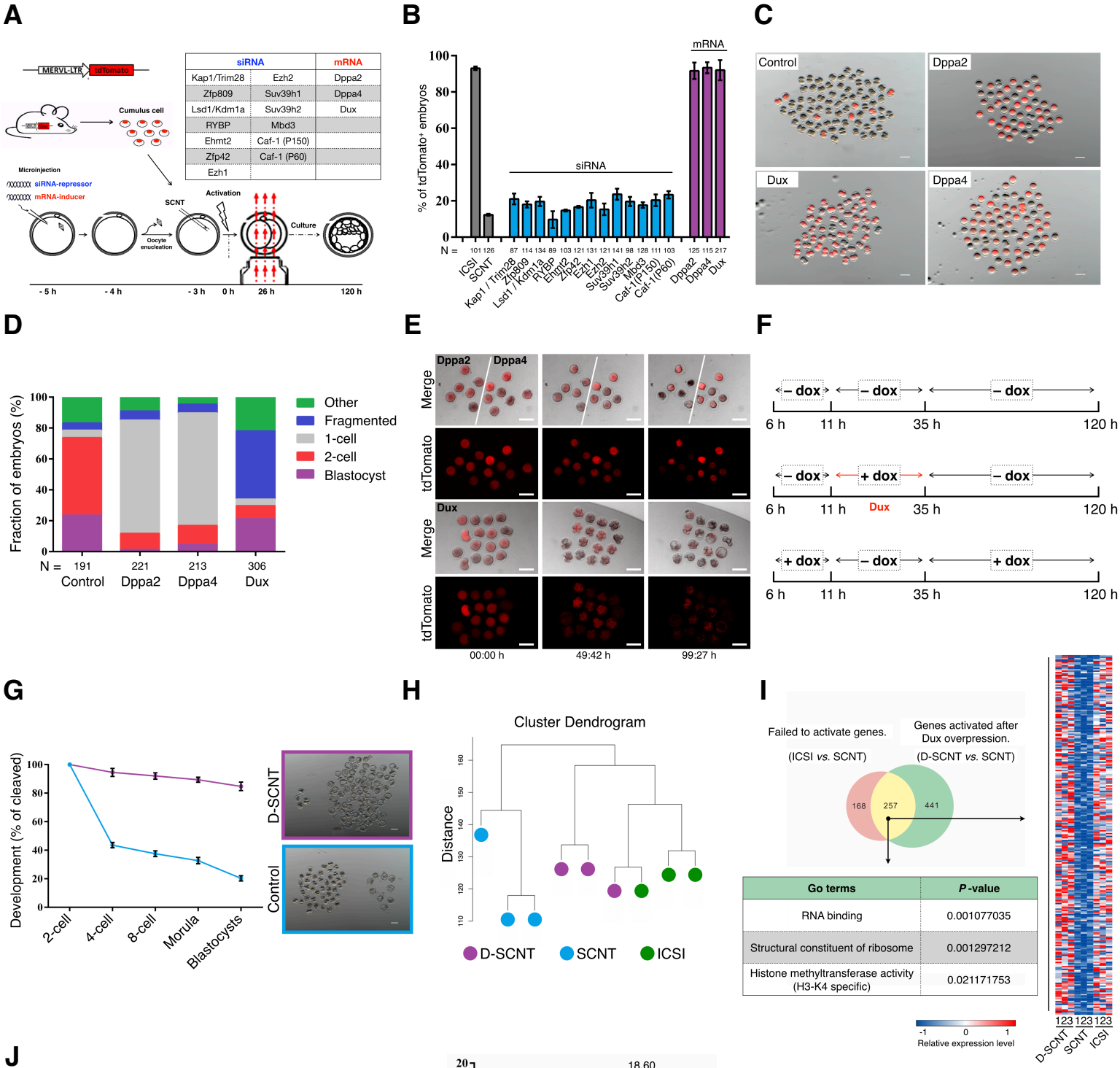
A
MERVL-LTR
tdTomato
Cumulus cell
Microinjection
siRNA-repressor
mRNA-inducer
SCNT
Activation
Oocyte enucleation
Culture
- 5 h
- 4 h
- 3 h
0 h
26 h
120 h
siRNA
mRNA
Kap1/Trim28
Zfp809
Lsd1/Kdm1a
RYBP
Ehmt2
Zfp42
Ezh1
Ezh2
Suv39h1
Suv39h2
Mbd3
Caf-1 (P150)
Caf-1 (P60)
Dppa2
Dppa4
Dux
B
% of tdTomato+ embryos
N =
ICSI
SCNT
C
Control
Dppa2
Dux
Dppa4
D
Fraction of embryos (%)
Other
Fragmented
1-cell
2-cell
Blastocyst
N =
191
221
213
306
Control
Dppa2
Dppa4
Dux
E
Merge
tdTomato
00:00 h
49:42 h
99:27 h
F
– dox
+ dox
6 h
11 h
35 h
120 h
G
Development (% of cleaved)
2-cell
4-cell
8-cell
Morula
Blastocysts
D-SCNT
Control
H
Cluster Dendrogram
Distance
D-SCNT
SCNT
ICSI
I
Failed to activate genes.
(ICSI vs. SCNT)
Genes activated after Dux overexpression.
(D-SCNT vs. SCNT)
168
257
441
Go terms
P-value
RNA binding
0.001077035
Structural constituent of ribosome
0.001297212
Histone methyltransferase activity (H3-K4 specific)
0.021171753
Relative expression level
J
SCNT
D-SCNT
% of 2-cell transferred
1.01
10.71
7.81
18.60
12.24
K-SCNT
D-Si-SCNT
K-Si-SCNT

Fig.2

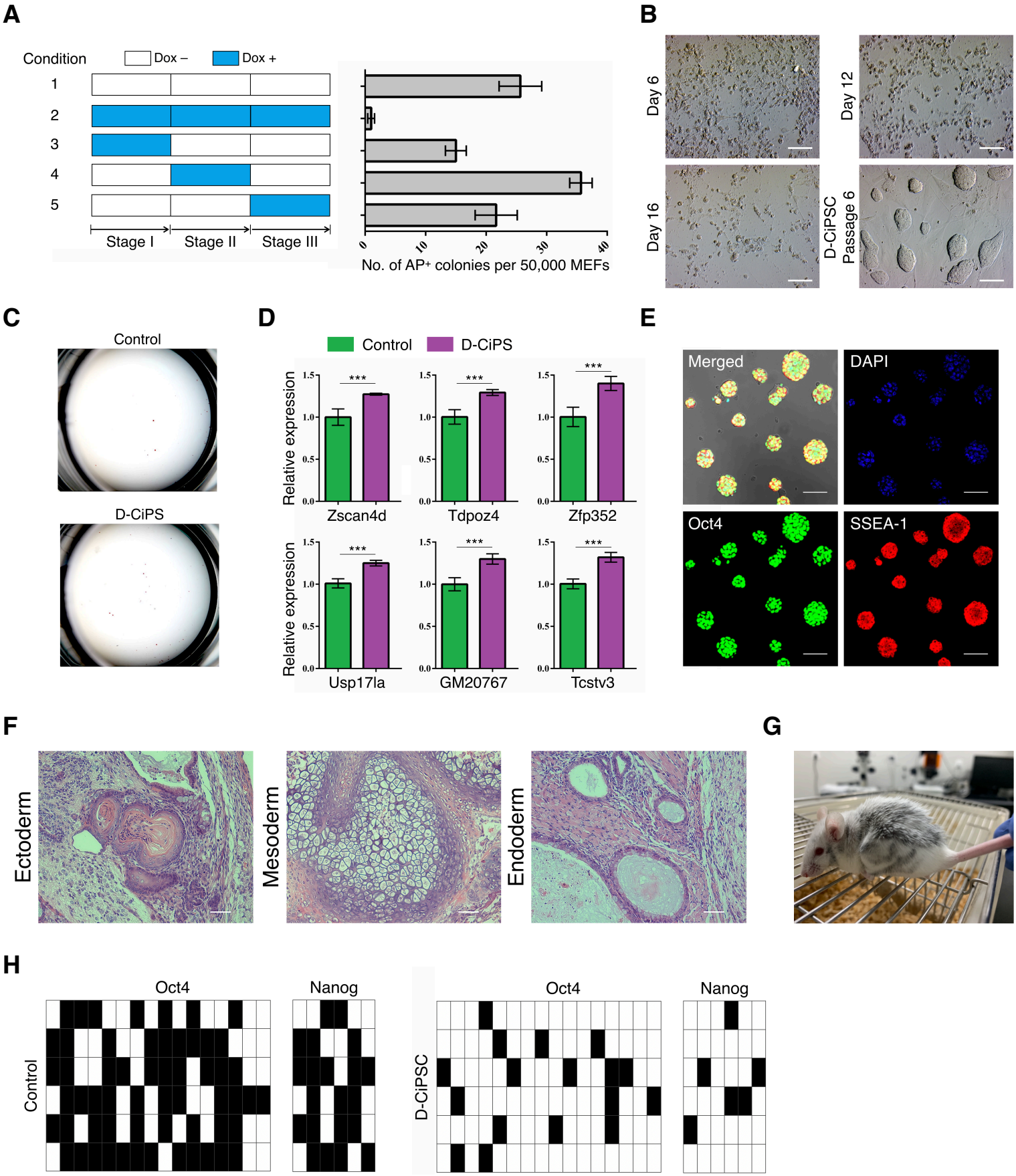
A
Condition
Dox –
Dox +
1
2
3
4
5
Stage I
Stage II
Stage III
0
10
20
30
40
No. of AP+ colonies per 50,000 MEFs
B
Day 6
Day 12
Day 16
D-CiPSC Passage 6
C
Control
D-CiPS
D
Control
D-CiPS
Relative expression
1.5
1.0
0.5
0.0
***
Zscan4d
Tdpoz4
Zfp352
Usp17la
GM20767
Tcstv3
E
Merged
DAPI
Oct4
SSEA-1
F
Ectoderm
Mesoderm
Endoderm
G
H
Oct4
Nanog
Control
D-CiPSC